4464–4474 *Nucleic Acids Research, 2011, Vol. 39, No. 10* *Published online 29 January 2011*
doi:10.1093/nar/gkr030

Structure of p300 bound to MEF2 on DNA reveals a mechanism of enhanceosome assembly

Ju He[1,3], Jun Ye[2], Yongfei Cai[1], Cecilia Riquelme[3], Jun O. Liu[4,5], Xuedong Liu[3], Aidong Han[1,*] and Lin Chen[2,6,*]

[1]MOE Key Laboratory for Cell Biology, School of Life Sciences, Xiamen University, Xiamen, Fujian 361005, China, [2]Department of Biological Sciences, Molecular and Computational Biology, Norris Comprehensive Cancer Center, Keck School of Medicine, University of Southern California, Los Angeles, CA 90089, USA, [3]Department of Chemistry and Biochemistry, University of Colorado at Boulder, Boulder, CO 80309, [4]Department of Pharmacology, [5]Department of Neuroscience, Johns Hopkins University School of Medicine, Baltimore, MD 21205, USA and [6]Key Laboratory of Cancer Proteomics of Chinese Ministry of Health, Xiangya Hospital, Central South University, 87 Xiangya Road, Changsha 410008, Hunan, China

Received November 18, 2010; Revised January 11, 2011; Accepted January 12, 2011

ABSTRACT

Transcription co-activators CBP and p300 are recruited by sequence-specific transcription factors to specific genomic loci to control gene expression. A highly conserved domain in CBP/p300, the TAZ2 domain, mediates direct interaction with a variety of transcription factors including the myocyte enhancer factor 2 (MEF2). Here we report the crystal structure of a ternary complex of the p300 TAZ2 domain bound to MEF2 on DNA at 2.2Å resolution. The structure reveals three MEF2:DNA complexes binding to different sites of the TAZ2 domain. Using structure-guided mutations and a mammalian two-hybrid assay, we show that all three interfaces contribute to the binding of MEF2 to p300, suggesting that p300 may use one of the three interfaces to interact with MEF2 in different cellular contexts and that one p300 can bind three MEF2:DNA complexes simultaneously. These studies, together with previously characterized TAZ2 complexes bound to different transcription factors, demonstrate the potency and versatility of TAZ2 in protein–protein interactions. Our results also support a model wherein p300 promotes the assembly of a higher-order enhanceosome by simultaneous interactions with multiple DNA-bound transcription factors.

INTRODUCTION

CBP and p300 are transcription co-activators of diverse gene expression programs (1). Their essential roles have been demonstrated by genetic studies and diseases associated with mutations in CBP/p300. Mice deficient in p300 lack cardiomyocyte proliferation and muscle-specific gene expression (2), whereas elevated p300 levels lead to myocardial hypertrophy (3). Mutations in CBP cause Rubinstein–Taybi Syndrome, a neurological disorder characterized by severe mental retardation (4). Disruptions of CBP and p300 regulation and function have also been linked to numerous cancers (5). CBP/p300 enhances transcription by facilitating the assembly of activating transcription complexes at the promoter and by modifying chromatin structure through its histone acetyltransferase (HAT) activity that can also modify non-histone proteins. These large nuclear proteins do not bind DNA but contain multiple domains capable of interacting with a variety of transcription factors (6), including the KIX domain that binds CREB and a number of cysteine–histidine rich regions (CH1–3), each of which binds directly to a large number of proteins (7). The CH3 region, which contains the TAZ2 domain, has been shown to interact with more than 20 proteins including viral protein E1A and host transcription factor p53 (8–18). Thus, CBP/p300 is extremely versatile in engaging numerous transcription factors to regulate gene expression (19–21). However, the molecular basis for this remarkable versatility is not well understood.

*To whom correspondence should be addressed. Tel: 213 821 4277; Fax: 213 740 8631; Email: linchen@usc.edu
Correspondence may also be addressed to Aidong Han. Email: ahan@xmu.edu.cn
Present address:
Ju He, Department of Pharmacology, University of Colorado at Denver, Aurora, CO 80045.

The authors wish it to be known that, in their opinion, the first two authors should be regarded as joint First Authors.

Extensive studies have established MEF2 as a major transcription factor partner of CBP/p300 in muscle, neurons and T cells (22–26). MEF2 is a class of transcription factors highly conserved in eukaryotes (27,28). Earlier genetic studies have demonstrated a central role of MEF2 in myogenesis (29–32). It is now clear that the MEF2 proteins (MEF2A-D) have broad roles in the differentiation, proliferation, and survival/apoptosis of a wide range of cell types (28,33,34). MEF2 also serves as a key regulator of stress responses and adaptive programs in animals, including fiber-type switch of skeletal muscle, hypertrophic growth of heart and activity-dependent remodeling of neuronal circuitry (35–39).

MEF2 turns on and off gene expression in a calcium-dependent manner (40). In the resting state, MEF2 recruits co-repressors such as Cabin1/Cain and histone deacetylases (HDAC) to specific loci of the genome to inhibit the expression of target genes (41–48). Upon activation, the co-repressors dissociate from MEF2 via calcium-dependent mechanisms (33,40,49–52); the DNA-bound MEF2 subsequently interacts with other calcium-activated transcription factors (e.g. NFAT and CREB) and recruits co-activators such as CBP/p300 and myocardin to activate transcription (1,2,22–26,53,54). The HDACs and CBP/p300 also regulate the transcriptional activity of MEF2 directly by controlling the acetylation state of specific lysine residues of MEF2 (55,56). The overall transcription state of MEF2-bound promoters is tightly controlled by signal-dependent protein–protein interactions between MEF2 and different co-regulators. Establishing how MEF2 interacts with these co-regulators will be a key to understanding the mechanisms of MEF2-regulated transcription.

The MEF2 family of transcription factors shares a highly conserved domain at the N-terminus, known as the MADS-box/MEF2 domain that mediates DNA binding, dimerization and protein–protein interactions with a variety of protein partners, including transcriptional co-repressors. Systematic structural studies reveal that a short amphipathic helix conserved in Cabin1 and class IIa HDACs (HDAC4, 5, 7 and 9) (referred to as MEF2-binding motif hereafter) binds a hydrophobic groove of MEF2 (53,57,58). These studies established a structural model for co-repressors to bind to MEF2 through their core interaction domains. Here, we characterized the interactions between MEF2 and its co-activator p300 by structural and biochemical analyses. These studies reveal the first atomic model of sequence-specific recruitment of transcription co-activator p300 by a DNA-bound transcription factor and provide new insights into the p300-mediated enhanceosome assembly.

MATERIALS AND METHODS

Materials

DNA plasmids of human MEF2A, Gal4-luciferase reporter, Gal4-MEF2D were kindly provided by Dr Xiangjiao Yang (McGill University). pET28a, pET30b and Rosetta BL21(DE3) pLysS competent cells were purchased from Novagen. Primers (for cloning) and oligo (for crystallization) were ordered from Integrated DNA Technologies (IDT). Glutathione-Sepharose beads, Sp sepharose, MonoS and Superdex 200HR were purchased from GE healthcare. *In vitro* transcription/translation kit was purchased from Promega and ^{35}S-Met was from Pierce. The mutations were generated using Quickchange mutagenesis kit (Stratagene). Lipofectamine 2000 was purchased from Invitrogen. Dual-luciferase reporter assay kit was from Promega. HeLa cells (ATCC) were grown in DMEM containing 10% fetal bovine serum. Other chemicals and reagents were purchased from Sigma.

Protein expression and purification

Human MEF2A (1–95) was expressed and purified as described previously (53). Briefly, pET30b-MEF2A (1–95) was transferred into BL21(DE3) pLysS Rosetta cells. The cells were induced at room temperature for 5 h. The induced cells were lysed by sonication in the lysis buffer (50 mM HEPES, pH 7.6, 300 mM NaCl, 1 mM EDTA, 1 mM DTT, 10% glycerol, protease inhibitors cocktails). The lysate was cleared by high-speed centrifugation and applied to Sp Sepherase column. Fractions containing MEF2 were pooled and further purified by superdex 200HR column using the buffer (10 mM HEPES, pH 7.6, 250 mM NaCl, 1 mM EDTA, 1 mM DTT).

The TAZ2 domain of human p300 (1726–1837) was cloned into pET28a. Based on the NMR structure of the CBP TAZ2 domain (59), the four cysteines (Cys1738, 1746, 1789 and 1790) not involved in zinc coordination were mutated to serine for better stability. The construct was transferred into Rosetta BL21(DE3) pLysS and induced at room temperature for 5 h with additional 150 μM $ZnSO_4$ in the medium. The cells were lysed by sonication. The p300 TAZ2 domain was first purified by Ni-NTA Agarose (QIAGEN) and eluted in 15 mM HEPES7.6, 1 M NaCl, 15 mM β-mercaptoethanol and 100 mM Imidazole. The imidazole was removed by dialysis and His-tag was cleaved off by thrombin. The p300 domain was further purified by MonoS, followed by superdex 200 HR in the running buffer of 10 mM HEPES pH 7.6, 25 mM NaCl, 0.4 M NH_4OAc, 2 mM DTT and 10 μM $ZnSO_4$.

Crystallization

The complex was prepared by mixing purified DNA, MEF2 dimer and the p300 TAZ2 domain in the superdex 200 HR running buffer (see above). The initial stoichiometry was 1:1:1 but after several rounds of optimization with various crystallization conditions and molar ratios of the complex composition, the best crystals came from complexes prepared by mixing 0.15 mM double stranded DNA, 0.3 mM MEF2 dimer and 0.9 mM p300 TAZ2 domain. The complex crystals were grown by the hanging drop method against a reservoir solution of 50 mM BTP pH 6.3, PEG 1K 16% and 2 mM DTT at 17°C.

Data collection and structure determination

The crystals were transferred into the cryo-buffer of 32% PEG 1K and 50 mM BTP pH 6.3 and flash frozen in liquid nitrogen. The data were collected in Advanced Light Source (ALS 8.2.1, Berkeley). Data were processed by HKL2000 (60). The p300:MEF2:DNA complex structure was solved by the molecular replacement method using the MEF2A:DNA crystal structure as a partial search model in Phaser (61,62). The initial search by molecular replacement located three MEF2:DNA complexes in the asymmetric unit. Electron density calculated using phases generated from the partial model revealed clearly the position of the p300 TAZ2 domain. Model building was carried out in O and Coot (63,64). The refinement was carried out using CNS (65,66) and the model was analyzed using programs from CCP4 (67). The Ramachadran plot of the final model has 96.7% of residues in the favorite region and 3.3% of residues in the allowed region and no residue in the disallowed region. All figures were prepared in Pymol (The Pymol Molecular Graphics System, DeLano Scientific LLC).

GST-pulldown

The TAZ2 fragments were expressed as GST fusion proteins. The proteins were purified by GST affinity column and gel filtration in the S200 buffer (50 mM HEPES, pH 7.6, 300 mM NaCl, 1 mM DTT, 10% glycerol and protease inhibitor cocktail). The quality and concentration of the proteins were checked by SDS–PAGE. The full-length MEF2A was prepared using an *in vitro* translation kit and labeled with ^{35}S-MET. The mixtures of labeled MEF2A and purified GST-p300 fusion proteins were incubated with GST beads for 1 h at 4°C, followed by three times wash using the same S200 buffer. The beads were collected for SDS–PAGE analysis followed by exposure to X-ray film.

Luciferase reporter assay

A plasmid was constructed to express the p300 TAZ2 domain (1721–1837) fused to the N terminal end of VP16 (Figure 5A). MEF2-Gal4 and Gal4 reporter plasmids were described by Gregoire and Yang (68). All these expression constructs were co-transfected to HeLa cells using lipofectamine 2000 or calcium phosphate. The experiments were performed in triplicate, and luciferases were measured using the dual-luciferase reporter assay kit according to manufacturer's instructions. Briefly, 20 µl of cell lysate was transferred to a luminometer tube predispensed with 100 µl of Luciferase Assay Reagent II (LARII), and luminescence of firefly luciferase was measured by a Luminometer (Berthold). Then, 100 µl of Stop & Glo Reagent was added to the same tube and the light emission of renilla luciferase was recorded. Results are presented as activity ratios of firefly over renilla luciferases.

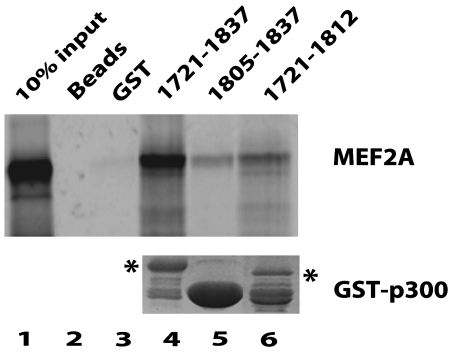

Figure 1. *In vitro* binding assay of the interaction between the p300 TAZ2 domain and MEF2A. Top panel: binding of the ^{35}S-labeled MEF2A to various GST-TAZ2 fusion proteins. Lane 2 was MEF2A with beads only. Lane 3 was GST only protein. Bottom panel: GST-TAZ2 fusion proteins used in the top panel were analyzed by SDS–PAGE. The non-degraded fusion protein bands are indicated by stars.

RESULTS

p300 TAZ2 domain binds the MADS-box/MEF2 domain

The interaction between MEF2 and p300 was analyzed previously by several reports (25,26,69). These studies revealed that the MADS-box/MEF2 domain of MEF2 (amino acids 1–95) and a C-terminal region of p300 (amino acids 1572–1868) were necessary and sufficient to mediate p300 and MEF2 interaction. We confirmed this result by GST pull-down assay using individually purified proteins. By deletion analyses, we narrowed down the MEF2-binding region in p300 to a fragment that encompasses residues 1721–1837 (Figure 1, lane 4). This fragment corresponds to the TAZ2 domain of the CH3 region (amino acids 1725–1812) and a C-terminal extension (amino acids 1813–1837) with unknown function. We will refer this fragment (amino acids 1721–1837) as the TAZ2 domain hereafter. We previously hypothesized that the C-terminal extension might bind MEF2 analogously to class IIa HDACs and Cabin1 (58). However, further deletion studies revealed that while p300 (1805–1837) did bind MEF2 (Figure 1, lane 5), its affinity for MEF2 appeared to be much lower than that of p300 (1721–1837) (Figure 1, lanes 4 and 5). Moreover, the core TAZ2 domain of p300 (1721–1812) retained partial binding activity for MEF2 (Figure 1, lane 6). We also analyzed the interaction between p300 (1721–1837) and MEF2A (1–95) using electrophoresis mobility shift assay (EMSA), surface plasmon resonance (SPR), multi-angle light scattering (MALS), mass spectrometry and fluorescence anisotropy. While these experiments confirmed the binding of p300 (1721–1837) and MEF2A (1–95) in solution, quantitative analysis of binding constant and stoichiometry was complicated by the fact that the complex appears to be in equilibrium between several species (data not shown). Moreover, the p300 TAZ2 domain alone showed high background binding to DNA, making the full titration of the MEF2:DNA complex by high concentration of TAZ2 difficult.

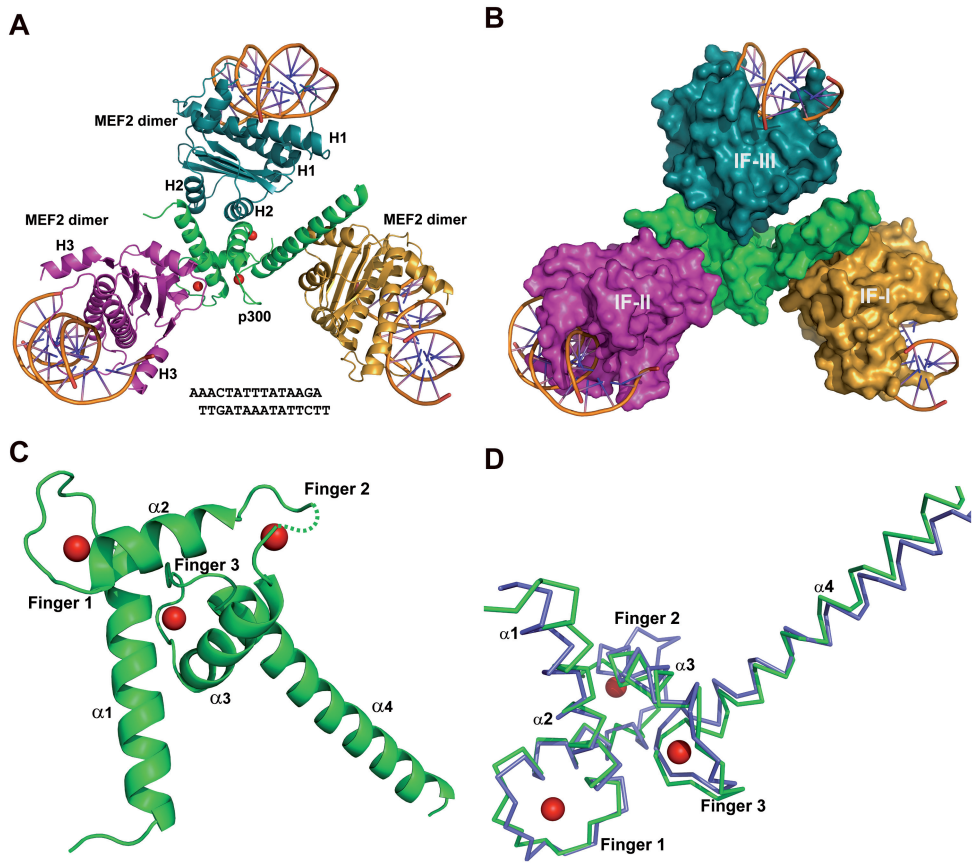

Figure 2. Structure of the p300 TAZ2 domain bound to MEF2 on DNA. (**A**) Overall structure in ribbon style. The MEF2 dimers are colored in yellow, magenta and blue, respectively; p300 is in green; the DNA backbone is shown in gold and its sequence is listed below. The secondary structural elements of one MEF2 dimer are labeled. (**B**) Protein binding interfaces: the proteins in the complex are shown in surface model and colored as in **A**. The three protein–protein interaction interfaces are labeled as IF-I, IF-II and IF-III. (**C**) Zoom-in view of the p300 TAZ2 domain. The four helices (α1–α4) and three zinc fingers (red spheres) are indicated. Part of the second zinc binding loop is disordered and labeled in a dashed line. (**D**) Superposition of the p300 TAZ2 domain in the MEF2-bound complex (green) with the unbound form (blue, 3IO2) (70).

Nevertheless, our biochemical analyses suggest that p300 binds MEF2 significantly differently from Cabin1 and class IIa HDACs in that p300 uses a larger domain instead of a short helix.

Crystallographic analysis of the p300:MEF2:DNA complex

In order to analyze the details of p300:MEF2 interaction, we crystallized a complex between p300 (1726–1837) and MEF2A (1–95) on DNA. Our initial crystallization was hindered by the instability of p300 (1726–1837) due to the large number of cysteine residues in this region. Based on the NMR structure of the CBP TAZ2 domain (59), we mutated four cysteine residues (Cys1738, 1746, 1789 and 1790) that do not coordinate with zinc to serine. The cysteine-mutated p300 TAZ2 domain showed much improved stability and retained the same ability to bind MEF2 as the wild-type protein (data not shown). Using this engineered p300 (1726–1837) together with MEF2A (1–95) and a double stranded oligonucleotide containing the consensus MEF2 binding element (see Figure 2A below), we successfully crystallized the p300:MEF2:DNA complex. The crystals diffracted to 2.2Å. The statistics of data collection and structure refinement are summarized in Table 1.

Overall structure of the p300:MEF2:DNA complex

The overall shape of the complex resembles a trefoil with the p300 TAZ2 domain in the center and the MEF2 dimer:DNA complexes at the leaf positions (Figure 2A). The core of the p300:MEF2:DNA complex is assembled through extensive helical packing that involves a total of 10 helices from the TAZ2 domain and the MADS-box/MEF2 domain (Supplementary Figure S1). The three MEF2 dimer:DNA complexes bind the p300 TAZ2 domain via three distinct and non-overlapping interfaces: Interface I (IF-I), Interface II (IF-II) and Interface III (IF-III), respectively (Figure 2B). The buried solvent accessible surface areas for these interfaces are: IF-I = 1213.8A^2, IF-II = 1223.1A^2 and IF-III = 1117.0A^2. The p300 TAZ2 domain in the complex is composed of four helices, α1 (amino acids 1727–1746), α2 (amino acids 1758–1766), α3 (amino acids 1782–1793) and α4 (amino acids 1806–1833) that pack against each other (Figure 2C). The structure is further stabilized by three zinc ions that are chelated between α1–α2 (Finger 1),

Table 1. Data collection and refinement statistics

Space group	P 2_1 2_1 2_1
Unit cell parameters (Å)	a = 74.85Å, b = 90.93Å, c = 144.8Å
Resolution (Å)	30.0–2.09 (2.16–2.09)[a]
Reflections (Total/unique)	1317602/59524
$I/\sigma(I)$[b]	27.3 (1.95)
R_{sym} (%)[c]	8.7 (70.9)
Completeness (%)	100 (100)
Refinement	
Resolution (Å)	29.666–2.192 (2.217–2.192)
Reflections	49213 (4536)
Completeness (%)	95.698
R (%)[d]	22.13 (25.62)
R_{free} (%)	27.16 (35.15)
Model quality	
RMSD bond length (Å)[e]	0.008
RMSD bond angles (°)	1.400
Overall B-factor (Å^2)	36.0
Number of total atoms[f]	7089
Protein atoms	5302
Nucleic acid atoms	1787
Ions	3
H2O	238

[a]The data for the highest resolution shell are shown in brackets.
[b]$I/\sigma(I)$—ratio of mean intensity to a mean standard deviation of intensity.
[c]$R_{sym} = \Sigma|I-<I>|/\Sigma I$, where I is the observed intensity, $<I>$ is the statistically weighted average intensity of multiple observations of symmetry-related reflections.
[d]$R_{factor} = \Sigma||F_o|-|F_c||/\Sigma|F_o|$, where F_o and F_c are observed and calculated structure factor amplitudes, respectively. R_{free} is calculated for a randomly chosen 10% of reflections.
[e]RMSD—root mean square deviation
[f]Number of protein atoms and nucleic acid atoms—the ordered region.

α2–α3 (Finger 2) and α3–α4 (Finger 3), respectively. Part of the second finger (amino acids 1772–1778) is disordered in the crystal and labeled in a dash line. Each zinc ion is bound by one histidine and three cysteines in an HCCC-type coordination.

The MADS-box/MEF2 domain in the complex forms an intertwined dimer; each monomer consists of helix H1 (amino acids 15–37), β strand S1 (amino acids 41–49), β strand S2 (amino acids 53–59), helix H2 (amino acids 62–70), β strand S3 (amino acids 76–80) and helix H3 (amino acids 82–90) (Figure 2A). For each MEF2 dimer, helix H1 and the N-terminal tail form the major DNA-binding surface that binds the double stranded DNA at the periphery of the complex, while the pair of H2 helices form the protein-binding interface with the TAZ2 domain in the center of the complex. All three MEF2 dimers show fully folded MADS-box/MEF2 domain (Figure 2A). The three MEF2A dimer:DNA complexes bound to the TAZ2 domain are nearly identical to each other and highly similar to the 'apo' MEF2A:DNA complex (Supplementary Figure S2). There is no interaction between the individual MEF2 dimer:DNA complexes.

Rigid p300 TAZ2 domain

Our TAZ2 structure reveals a protein fold that is very similar to the homologous TAZ2 domain of CBP first solved by NMR (59). The crystal structure of the unbound p300 TAZ2 domain has recently been reported (70). Superposition of the p300 TAZ2 domain in the unbound state with that in the MEF2-bound complex shows that the two structures are very similar, although the N-terminal end of α1 and the C-terminal end of α4 have slightly different trajectories (Figure 2D). The α2-α3 loop also displays significant differences due to different crystal packing interactions. The spatial arrangement of the four helices and the structure of the three zinc binding sites are highly conserved in the unbound state and in complexes with different protein partners, although the loops between the helices show a certain degree of variability due to different crystal packing and protein–protein interactions (9,14,16,59). A significant difference from the solution structure of the TAZ2 domain is that we observed an extended helix α4 in the crystal structure of the p300 TAZ2 domain (Figure 2C). This long helix α4 was also observed in a ligand-free TAZ2 structure (70). Overall, the structural comparisons suggest that the formation of the p300:MEF2:DNA complex involves largely rigid body docking interactions of the preformed MEF2A:DNA complex and the p300 TAZ2 domain.

Protein–protein interactions at Interface I

Interface I is formed between helix α4 of the TAZ2 domain and one of the MEF2 dimers. Here helix α4 of the TAZ2 domain packs diagonally between helices H2 of the MEF2 dimer. This arrangement is very similar to the binding of the amphipathic helix of Cabin1 and HDAC9 to MEF2, however, the exact positions of the helices are slightly different in different complexes (Figure 3A). Previously we showed that the binding of Cabin1 and HDAC9 to MEF2 induced a shift of helix H2 and conformational changes of the L2 loop between helix H2 and strand S3 (53,57,58). The L2 conformations of MEF2 bound to the p300 TAZ2 domain are indeed notably different from that seen in the Cabin1:MEF2 and HDAC9:MEF2 complexes (Figure 3A). The detailed interactions of IF-I share many features observed at the Cabin1:MEF2 and HDAC9:MEF2 interfaces (Figure 3B and C). *Leu1818* and *Leu1822* of p300 bind the hydrophobic groove of MEF2 similarly to homologous leucine residues in Cabin1 and HDAC9 (residues of p300 are italicized throughout the text) (57,58). Surrounding the hydrophobic interactions are numerous salt bridges and hydrogen bond networks. At the N-terminal end of TAZ2 α4, *Arg1814* engages in electrostatic interactions with Asp61 and Asp63 of MEF2, whereas *Gln1811*and *Gln1815* form hydrogen bonds with Asp63 and the main chain carbonyl of Thr70 of MEF2, respectively. Both *Gln1811*and *Gln1815* are also in van der Waals contact with Tyr69 of MEF2. At the C-terminal end of TAZ2 α4, *Arg1829* engages in electrostatic interactions with Asp61 and Asp63 of the other MEF2 monomer. Along the helix of TAZ2 α4, the long aliphatic side chains of *Arg1814*, *Gln1815, Gln1819* and *Arg1821* make extensive van der Waals contacts with residues of helix H2 of the MEF2 dimer. Here, *Gln1819* also forms a hydrogen bond with Thr70 while *Arg1821* forms a salt bridge with Glu71.

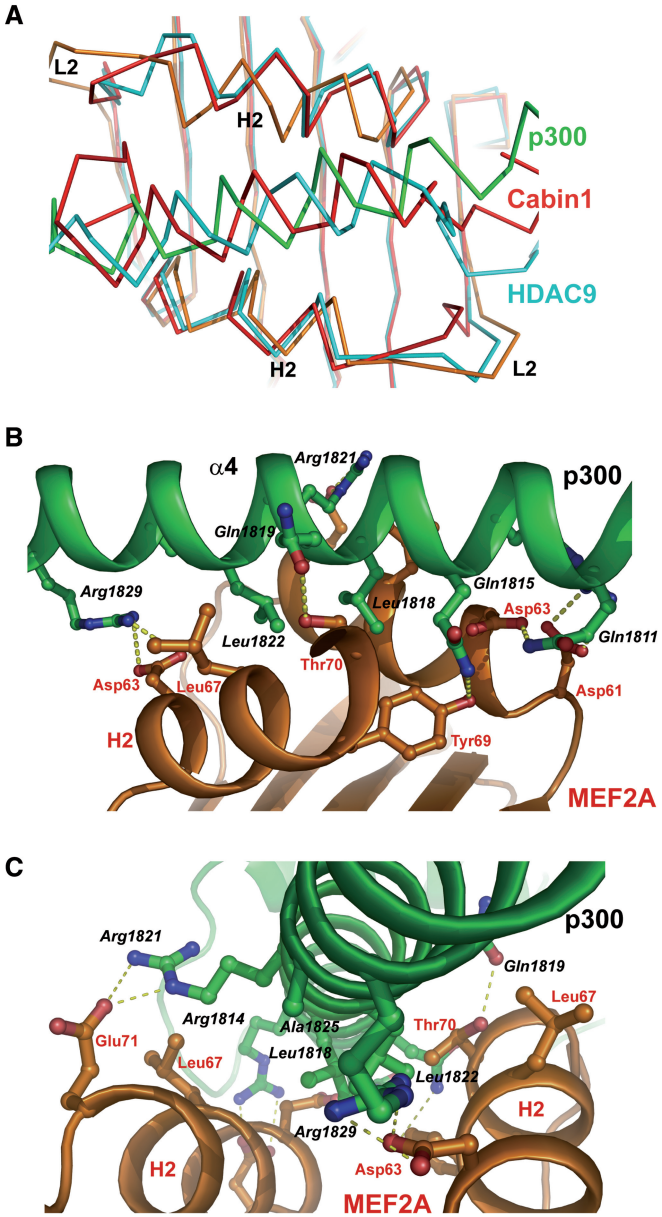

Figure 3. Protein–protein interactions at Interface I. (**A**) Structural comparison of Interface I (p300 in green and MEF2 in gold) with the Cabin1:MEF2:DNA complex (red) and the HDAC9:MEF2:DNA complex (cyan). The structures are superimposed by the Cα backbone of the β strands of the MEF2 core. (**B**) View from the side of helix α4 of the p300 TAZ2 domain. Interacting residues are shown in stick model. Throughout the illustrations, residues from p300 are italicized and labeled with black fonts while residues from MEF2 are labeled according to the protein color. (**C**) View from the C-terminal end of helix α4.

Overall, IF-I shows a remarkably similar binding mode to Cabin1 and HDAC9 as well as new features of protein–protein interactions.

Protein–protein interactions at Interface II

Interface II is formed between helix α1 and the first zinc loop of the TAZ2 domain and a second MEF2 dimer. Here, helix α1 of the TAZ2 domain lies above the two H2 helices of the MEF2 dimer at a cross angle of ~60° (Supplementary Figure S3). The interface is composed of two separated foci of binding interactions; the first being between the N-terminal part of the TAZ2 α1 helix and helix H2 of one MEF2 monomer (Figure 4A). *Met1725* and *Leu1733* of p300 and Leu67 of MEF2 form a central hydrophobic patch that is surrounded by a number of electrostatic and hydrogen bond interactions, including salt bridges between *Arg1737* and Asp63 and between *Arg1732* and Glu71. At the second binding site of IF-II, the C-terminal part of TAZ2 α1 helix and part of the first zinc loop interact with helix H2 of the other MEF2 monomer. *Leu1755* of p300 and Leu67 of MEF2 form the hydrophobic core. Leu67 also makes van der Waals contacts with *Gln1740* and *His1744*, while Glu71 makes hydrogen bonds with the main chain and side chain of Ser1757. The side chain of *Arg1737* and *Pro1756* also make van der Waals contacts with Thr70 and Glu71, respectively.

Protein–protein interactions at Interface III

Interface III is formed between helices α1 and α3 of the TAZ2 domain and a third MEF2 dimer. Here, α1 and α3 of the TAZ2 domain pack against helix H2 of each of the two MEF2 monomers, both in an approximately parallel orientation (Supplementary Figure S4). Similar to IF-II, IF-III is also composed of two separated foci of binding interactions. One is between helix α1 of the TAZ2 domain and helix H2 of one of the MEF2 monomers (Figure 4B). Here, *Pro1727*, *Gly1728*, *Ser1730* and *Arg1731* of p300 and Asp63, Lys64, Leu66, Leu67 and Thr70 of MEF2 engage in a pseudo knobs-into-holes type helix packing interaction. *Arg1731* also forms a hydrogen bond with Thr70. At the second binding site (Figure 4C), *Lys1783*, *Gln1784*, *Ala1787*, *Cys1790*, *Tyr1791* and *Lys1794* on the exposed face of p300 α3 form an extensive interface with Asp61, Asp63, Lys64, Leu67 and Glu71 on helix H2 of one of the MEF2 monomers. Most notably, *Cys1790* and *Tyr1791* of p300 and Leu67 of MEF2 form a hydrophobic patch, *Lys1783* and *Lys1794* engage in electrostatic interactions with Asp61 and Glu71, respectively. Overall, the binding modes of IF-II and IF-III are substantially different from that seen in the Cabin1:MEF2 complex and HDAC9:MEF2 complex, but both interfaces bury large solvent accessible surface areas and display good shape and chemical complementarity.

Biochemical analysis of the p300:MEF2 interaction

To test if the protein–protein interfaces seen in the crystal structure contribute to p300:MEF2 interaction, we analyzed a series of structure-guided mutations using a mammalian two-hybrid assay specifically designed for detecting the interaction between the p300 TAZ2 domain and the MADS-box/MEF2 domain in mammalian cells. Initially, we transfected a MEF2-responsive luciferase reporter with full-length p300 and MEF2 to detect MEF2-p300 interaction. These studies did not yield interpretable results due to high background, presumably caused by the endogenous MEF2 and p300. To overcome this problem, we adopted a mammalian

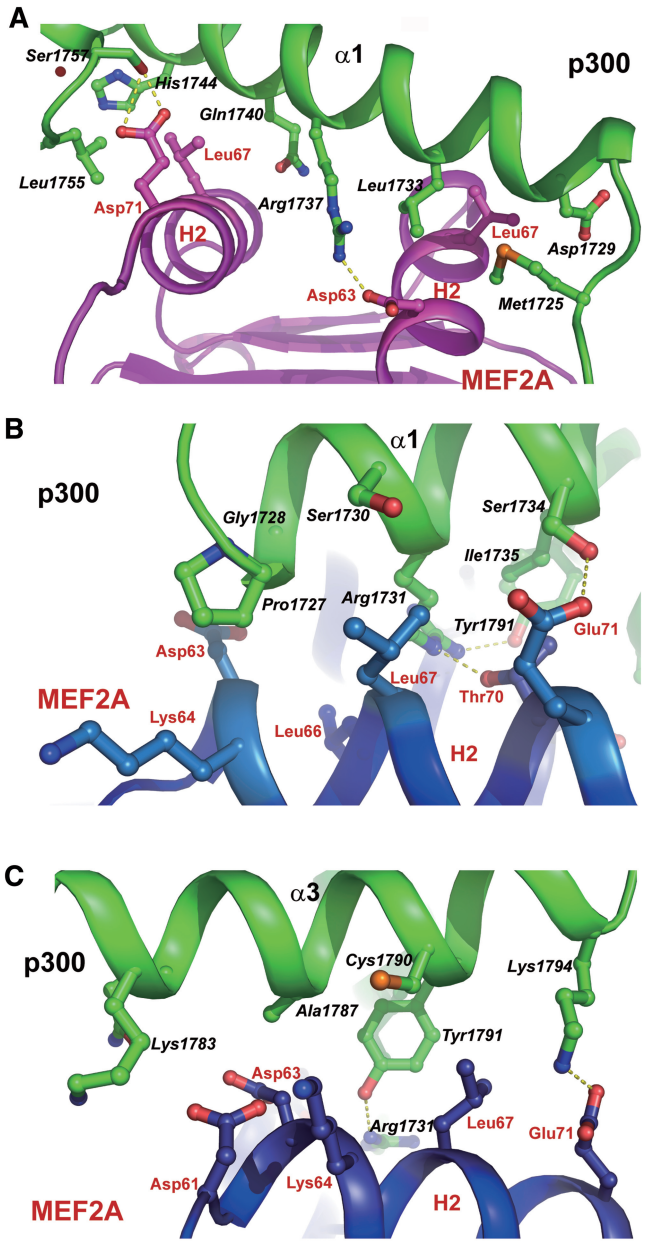

Figure 4. Protein–protein interactions at interfaces II and III. (**A**) The interaction network at Interface II. (**B**) Interactions at Interface III viewed from the side of helix α1. (**C**) Interactions at Interface III viewed from the side of helix α3.

two-hybrid assay by fusing MEF2 with the GAL4 DNA-binding domain (GAL4-MEF2) and the p300 TAZ2 domain with VP-16 (TAZ2-VP16) (Figure 5A). This setup allows us to detect the interaction between TAZ2 and MEF2 with minimal interference from endogenous factors. A potential caveat of this approach is that MEF2 is not directly bound to DNA whereas under physiological conditions p300 is recruited by DNA bound MEF2. However, we have previously shown that free MEF2 and DNA-bound MEF2 bind co-factors with similar affinities, suggesting that the structure of MEF2, at least in the MADS-box/MEF2 domain, is conserved between the free and DNA-bound forms (57). HeLa cells co-transfected with constructs of GAL4-MEF2 and TAZ2-VP16 together with a GAL4-driven reporter plasmid produced a strong signal comparable to that generated by the positive control of GAL4-VP16 (data not shown). At Interface I, the double mutation *Leu1818Ala/Leu1822Ala* caused a significant reduction of the luciferase signal, whereas mutation of *Gln1815Ala* and *Gln1815Tyr* had little effect (Figure 5B). These results suggest that the hydrophobic residues at the center of IF-I are important for binding, whereas residues at the periphery are more tolerable to mutations. At Interface II, double mutation *Leu1733Arg/Arg1737Ala* and triple mutation *Leu1733Ala/Arg1737Ala/Gln1740Ala* reduced the luciferase signal substantially, whereas the single mutation *Gln1740Ala* had only partial effect. Interestingly, the mutation *Gln1740Tyr* enhanced the luciferase signal, suggesting that the Tyrosine residue introduced at position 1740 may interact better with MEF2, presumably by inserting into the hydrophobic groove between helices H2. These mutational data are consistent with the structural features of IF-II and suggest that IF-II contributes to p300:MEF2 interaction in solution. At Interface III, mutation *Arg1731Ala* and *Tyr1791Ala* partially reduced the luciferase signal, which is consistent with the structural roles of these residues at IF-III. However, the double mutation *Arg1731Ala/Tyr1791Ala* enhanced the luciferase signal. The mechanism of this gain-of-function mutation is not clear. It is possible that the *Arg1731Ala/Tyr1791Ala* double mutant adopts a new way to bind MEF2 that is different than seen in the crystal structure. Taken together, these data suggest that protein–protein interactions observed at interfaces I, II and III contribute to the binding of the p300 TAZ2 domain to MEF2 in solution. For some of the mutations that showed strong effects in the luciferase assay, such as the double mutant *Leu1818Ala/Leu1822Ala* and *Leu1733Arg/Arg1737Ala*, our GST-pulldown also confirmed that the mutant proteins lost the binding to MEF2 *in vitro* (data not shown).

DISCUSSION

The crystal structure of the p300 TAZ2 domain reported by Miller *et al.* (59,70) reveals a new feature that is not seen in the previous NMR structure of the CBP TAZ2 domain, namely an extended helix α4. This unusually long helix makes no contacts with the rest of the TAZ domain but engages in extensive interactions with symmetry related molecules in crystal (70). It was not observed in the NMR structure of the same domain bound to p53 because a shorter p300 fragment (1723–1812) was used (14). However, the extended helix α4 was involved in extensive crystal packing interactions in the structure reported by Miller *et al.* (59,70), a question remains if the observed structure of helix α4 is a result of crystal packing. The p300 TAZ2 domain in our crystal structure reveals a similar extended helix α4, which, instead of making crystal contacts, engaged in extensive interactions with a MEF2 dimer at IF-I. This observation

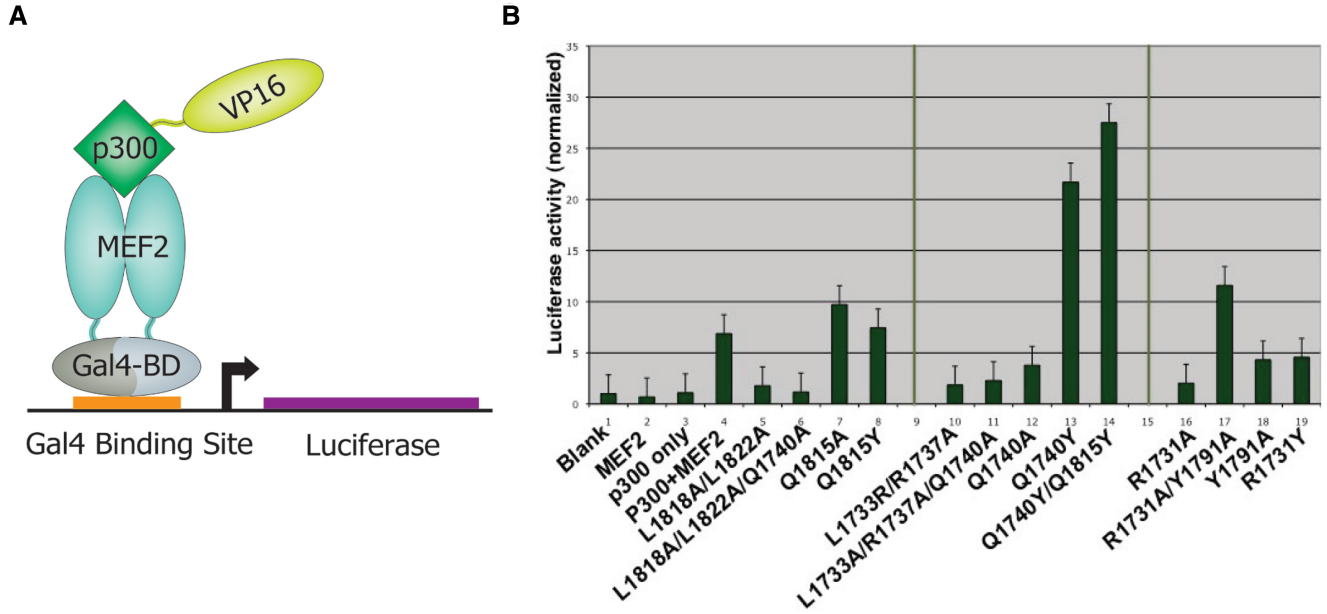

Figure 5. Structure-guided biochemical analyses of p300:MEF2 interactions. (**A**) Diagram of the biochemical assay. (**B**) Luciferase reporter assay of p300 TAZ2 mutants. Columns 1–3 are controls. Column 4 is from wild-type p300 and MEF2 interaction. Columns 5–8 are IF-I mutants, 10–14 are IF-II mutants and 16–19 are IF-III mutants. Column 6 is a combined mutant of IF-I and IF-II.

suggests that the structure of helix α4 is an intrinsic property of the p300 TAZ2 domain. Consistent with this view, CD analysis indicated that the C-terminal region of p300 TAZ2 domain forms alpha helix in solution (15). Our studies further suggest that a potential function of this long helix is to mediate protein–protein interactions with other proteins, including a variety of transcription factors, such as MEF2.

Based on the crystal structure of the Cabin1:MEF2:DNA complex and sequence homology, we have previously hypothesized that the region of p300 corresponding to residues *Leu1807* to *Gln1819* could form an amphipathic helix to bind MEF2 in a way similar to Cabin1 (58). Our structure reveals that this region of p300 indeed forms an alpha helix as part of α4, but it is packed against helix α3 and sterically blocked from MEF2 binding. Instead, MEF2 at IF-I binds to a hydrophobic patch on helix α4 that is centered around *Leu1818* and *Leu1822*. This hydrophobic patch has been noted in the unbound structure of the p300 TAZ domain, which mediates the majority of crystal packing interactions (70). Despite the shift of the predicted MEF2-binding site, the binding mode between MEF2 and the TAZ2 domain at IF-I is remarkably similar to that seen in the Cabin1:MEF2:DNA complex and the HDAC9:MEF2:DNA complex, whereas those at IF-II and III are significantly different from the canonical mode defined previously (57).

A frequently observed mode of co-factor recruitment in transcription complexes is binding-induced folding. Usually one protein with a stably folded domain presents a template for the binding and folding of its partner with intrinsically disordered regions. The TAZ2 domain serves as the binding site for the transcription activation domains of a number of transcription factors, including STAT1 and p53, which are disordered in solution and adopt a short helix to bind the hydrophobic surface between helices α1, α2 and α3 (14,16). The conserved region-1 (CR1) of the adenoviral protein E1A, which is unstructured in solution, also binds this region in a helical conformation (9). The binding sites for different factors on TAZ2 partially overlap, such that E1A can compete with p53 for p300 binding (9). The hydrophobic surface between helices α1, α2 and α3 is also a MEF2-binding site in the p300:MEF2 complex (IF-III). However, the binding of MEF2 to TAZ2 involves mostly rigid body docking without significant structural changes of either MEF2 or the TAZ2 domain.

CBP/p300 can acetylate specific lysine residues in MEF2 to enhance its DNA binding and transcriptional activity (56,71). The fact that the TAZ2 domain (amino acids 1721–1837) is adjacent to the HAT domain in p300 (amino acids 1066–1707) suggests that p300 could acetylate MEF2 within the same complex. It should be noted that the transcription activation domain of MEF2, which is located beyond the MADS-box/MEF2 domain at the C-terminal end, might interact with p300 at additional regions. Thus in the context of full-length proteins, p300 and MEF2 may bind each other through multiple contacts and a variety of binding modes.

CBP/p300-mediated enhanceosome assembly has long been hypothesized (19–21). Our structure provides the first example where a p300 domain is directly recruited to DNA by a DNA-bound, sequence-specific transcription factor. A surprising finding is that MEF2 binds the p300 TAZ2 domain at three distinct and non-overlapping surfaces, leading to an assembly of a higher-order enhanceosome structure wherein three DNA-bound MEF2 dimers are 'attracted' to different faces of the

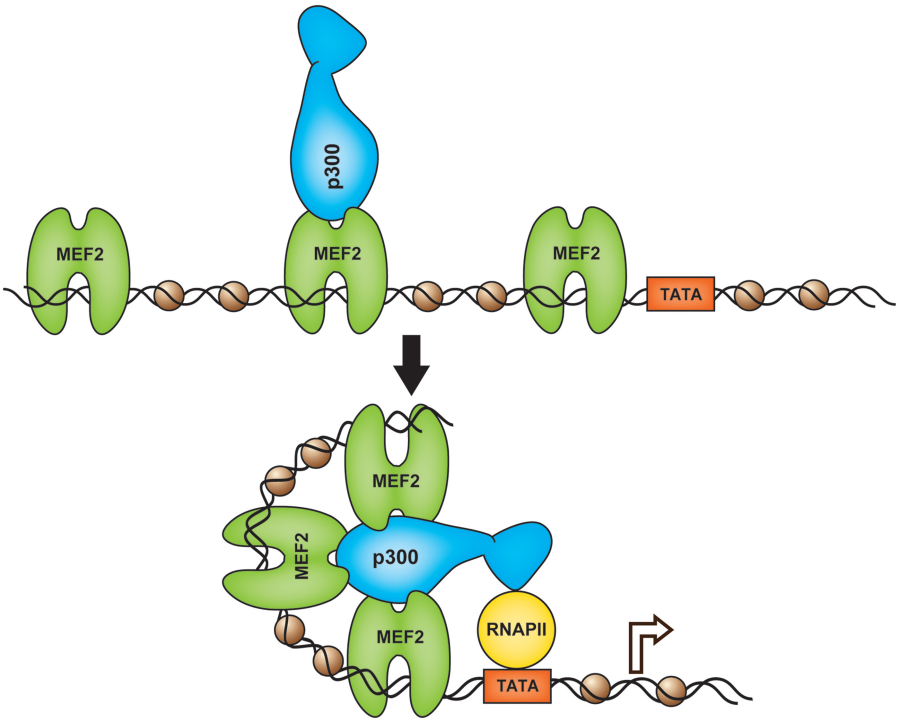

Figure 6. A hypothetical enhanceosome model. Multiple MEF2 dimers bind to numerous sites in the enhancer/promoter region of a targeted gene. Brown balls represent the nucleosomes. p300 is recruited to one MEF2 dimer:DNA complex to initiate the assembly of the activation complex. Subsequent binding of p300 to other two MEF2 dimer:DNA complexes induces a looping of DNA and the assembly of an enhanceosome.

TAZ2 domain. This has two implications for the transcriptional regulation by p300 and MEF2. First, the TAZ2 domain from one p300 molecule could interact with three MEF2 dimers bound to DNA, thereby promoting the assembly of higher-order structures in the promoter and long-range interactions of DNA-bound MEF2 complexes (Figure 6). Our structure does not impose any spatial constraint between the different MEF2 sites as long as they are well separated so the intervening sequences could be looped out. In fact, the MEF2 binding sites could even come from different chromosomes. In this regard, recent ChIP-on-chip studies reveal that MEF2 bind a much larger number of sites in the genome than previously thought, and that most MEF2-targeted promoters contain multiple MEF2 binding sites that are separated far from each other (often more than several kilobases) (31). Second, as discussed above, the TAZ domain can interact with a variety of other proteins, including different transcription factors. The fact that MEF2 can bind three distinct sites on TAZ2 opens up the possibility that MEF2 may bind one of the three sites in a given promoter context, leaving room for the binding of other transcription factors to the TAZ2 domain. This versatility of p300:MEF2 interaction may facilitate combinatorial control of transcription regulation between MEF2 and other transcription factors. Future studies are needed to further address these questions, for example, by analyzing the effect of mutations at different interfaces on the expression of specific subsets of MEF2-targeted genes.

ACCESSION NUMBER

Coordinates and structure factors have been deposited in the Protein Data Bank with accession number 3P57.

SUPPLEMENTARY DATA

Supplementary Data are available at NAR Online.

ACKNOWLEDGEMENTS

The authors would like to thank Dr Xiang-Jiao Yang (McGill University) for providing plasmids; Dr Xiaojiang Chen, Dr Yongheng Chen, Reza Kalhor and Nimanthi Jayathilaka for suggestions and helpful discussion; Mrs Chen Wang in purification of p300 mutants and figure preparations; Michael Philips for proofreading the article; Dr Nickolas Chelyapov and USC NanoBiophysics Core Facility for help with Biacore and fluorescence anisotropy studies; Dr Joseph Lo of UCLA for Mass Spec studies; ALS BCSB staff members Corie Ralston, Peter Zwart, Christine Bertoldo and Kevin Royal for help with data collection.

FUNDING

National Institutes of Health, USA (HL076334, GM064642 and GM077320 to L.C. and GM83172 to X.J.); National Science Foundation of China (30840027 and 90919036 to A.H.); Fujian Science Advancing

Program (2009J1010 and Project 111). Funding for open access charge: Fujian Science advancing Program (2009J1010).

Conflict of interest statement. None declared.

REFERENCES

1. Goodman,R.H. and Smolik,S. (2000) CBP/p300 in cell growth, transformation, and development. *Genes Dev.*, **14**, 1553–1577.
2. Yao,T.P., Oh,S.P., Fuchs,M., Zhou,N.D., Ch'ng,L.E., Newsome,D., Bronson,R.T., Li,E., Livingston,D.M. and Eckner,R. (1998) Gene dosage-dependent embryonic development and proliferation defects in mice lacking the transcriptional integrator p300. *Cell*, **93**, 361–372.
3. Wei,J.Q., Shehadeh,L.A., Mitrani,J.M., Pessanha,M., Slepak,T.I., Webster,K.A. and Bishopric,N.H. (2008) Quantitative control of adaptive cardiac hypertrophy by acetyltransferase p300. *Circulation*, **118**, 934–946.
4. Petrij,F., Giles,R.H., Dauwerse,H.G., Saris,J.J., Hennekam,R.C., Masuno,M., Tommerup,N., van Ommen,G.J., Goodman,R.H., Peters,D.J. *et al*. (1995) Rubinstein-Taybi syndrome caused by mutations in the transcriptional co-activator CBP. *Nature*, **376**, 348–351.
5. Giles,R.H., Peters,D.J. and Breuning,M.H. (1998) Conjunction dysfunction: CBP/p300 in human disease. *Trends Genet.*, **14**, 178–183.
6. Dyson,H.J. and Wright,P.E. (2005) Intrinsically unstructured proteins and their functions. *Nat. Rev. Mol. Cell Biol.*, **6**, 197–208.
7. Radhakrishnan,I., Perez-Alvarado,G.C., Parker,D., Dyson,H.J., Montminy,M.R. and Wright,P.E. (1997) Solution structure of the KIX domain of CBP bound to the transactivation domain of CREB: a model for activator:coactivator interactions. *Cell*, **91**, 741–752.
8. Arany,Z., Newsome,D., Oldread,E., Livingston,D.M. and Eckner,R. (1995) A family of transcriptional adaptor proteins targeted by the E1A oncoprotein. *Nature*, **374**, 81–84.
9. Ferreon,J.C., Martinez-Yamout,M.A., Dyson,H.J. and Wright,P.E. (2009) Structural basis for subversion of cellular control mechanisms by the adenoviral E1A oncoprotein. *Proc. Natl Acad. Sci. USA*, **106**, 13260–13265.
10. Gu,W., Shi,X.L. and Roeder,R.G. (1997) Synergistic activation of transcription by CBP and p53. *Nature*, **387**, 819–823.
11. Avantaggiati,M.L., Ogryzko,V., Gardner,K., Giordano,A., Levine,A.S. and Kelly,K. (1997) Recruitment of p300/CBP in p53-dependent signal pathways. *Cell*, **89**, 1175–1184.
12. Teufel,D.P., Bycroft,M. and Fersht,A.R. (2009) Regulation by phosphorylation of the relative affinities of the N-terminal transactivation domains of p53 for p300 domains and Mdm2. *Oncogene*, **28**, 2112–2118.
13. Ferreon,J.C., Lee,C.W., Arai,M., Martinez-Yamout,M.A., Dyson,H.J. and Wright,P.E. (2009) Cooperative regulation of p53 by modulation of ternary complex formation with CBP/p300 and HDM2. *Proc. Natl Acad. Sci. USA*, **106**, 6591–6596.
14. Feng,H., Jenkins,L.M., Durell,S.R., Hayashi,R., Mazur,S.J., Cherry,S., Tropea,J.E., Miller,M., Wlodawer,A., Appella,E. *et al*. (2009) Structural basis for p300 Taz2-p53 TAD1 binding and modulation by phosphorylation. *Structure*, **17**, 202–210.
15. Jenkins,L.M., Yamaguchi,H., Hayashi,R., Cherry,S., Tropea,J.E., Miller,M., Wlodawer,A., Appella,E. and Mazur,S.J. (2009) Two distinct motifs within the p53 transactivation domain bind to the Taz2 domain of p300 and are differentially affected by phosphorylation. *Biochemistry*, **48**, 1244–1255.
16. Wojciak,J.M., Martinez-Yamout,M.A., Dyson,H.J. and Wright,P.E. (2009) Structural basis for recruitment of CBP/p300 coactivators by STAT1 and STAT2 transactivation domains. *EMBO J.*, **28**, 948–958.
17. Wells,M., Tidow,H., Rutherford,T.J., Markwick,P., Jensen,M.R., Mylonas,E., Svergun,D.I., Blackledge,M. and Fersht,A.R. (2008) Structure of tumor suppressor p53 and its intrinsically disordered N-terminal transactivation domain. *Proc. Natl Acad. Sci. USA*, **105**, 5762–5767.
18. Teufel,D.P., Freund,S.M., Bycroft,M. and Fersht,A.R. (2007) Four domains of p300 each bind tightly to a sequence spanning both transactivation subdomains of p53. *Proc. Natl Acad. Sci. USA*, **104**, 7009–7014.
19. Courey,A.J. and Jia,S. (2001) Transcriptional repression: the long and the short of it. *Genes Dev.*, **15**, 2786–2796.
20. Lemon,B. and Tjian,R. (2000) Orchestrated response: a symphony of transcription factors for gene control. *Genes Dev.*, **14**, 2551–2569.
21. Vo,N. and Goodman,R.H. (2001) CREB-binding protein and p300 in transcriptional regulation. *J. Biol. Chem.*, **276**, 13505–13508.
22. Molkentin,J.D., Black,B.L., Martin,J.F. and Olson,E.N. (1995) Cooperative activation of muscle gene expression by MEF2 and myogenic bHLH proteins. *Cell*, **83**, 1125–1136.
23. Youn,H.D., Chatila,T.A. and Liu,J.O. (2000) Integration of calcineurin and MEF2 signals by the coactivator p300 during T-cell apoptosis [In Process Citation]. *EMBO J.*, **19**, 4323–4331.
24. Eckner,R., Yao,T.P., Oldread,E. and Livingston,D.M. (1996) Interaction and functional collaboration of p300/CBP and bHLH proteins in muscle and B-cell differentiation. *Genes Dev.*, **10**, 2478–2490.
25. Sartorelli,V., Huang,J., Hamamori,Y. and Kedes,L. (1997) Molecular mechanisms of myogenic coactivation by p300: direct interaction with the activation domain of MyoD and with the MADS box of MEF2C. *Mol. Cell. Biol.*, **17**, 1010–1026.
26. Slepak,T.I., Webster,K.A., Zang,J., Prentice,H., O'Dowd,A., Hicks,M.N. and Bishopric,N.H. (2001) Control of cardiac-specific transcription by p300 through myocyte enhancer factor-2D. *J. Biol. Chem.*, **276**, 7575–7585.
27. Gossett,L.A., Kelvin,D.J., Sternberg,E.A. and Olson,E.N. (1989) A new myocyte-specific enhancer-binding factor that recognizes a conserved element associated with multiple muscle-specific genes. *Mol. Cell. Biol.*, **9**, 5022–5033.
28. Potthoff,M.J. and Olson,E.N. (2007) MEF2: a central regulator of diverse developmental programs. *Development*, **134**, 4131–4140.
29. Bour,B.A., O'Brien,M.A., Lockwood,W.L., Goldstein,E.S., Bodmer,R., Taghert,P.H., Abmayr,S.M. and Nguyen,H.T. (1995) Drosophila MEF2, a transcription factor that is essential for myogenesis. *Genes Dev.*, **9**, 730–741.
30. Lilly,B., Zhao,B., Ranganayakulu,G., Paterson,B.M., Schulz,R.A. and Olson,E.N. (1995) Requirement of MADS domain transcription factor D-MEF2 for muscle formation in Drosophila. *Science*, **267**, 688–693.
31. Sandmann,T., Jensen,L.J., Jakobsen,J.S., Karzynski,M.M., Eichenlaub,M.P., Bork,P. and Furlong,E.E. (2006) A temporal map of transcription factor activity: mef2 directly regulates target genes at all stages of muscle development. *Dev. Cell*, **10**, 797–807.
32. Lovato,T.L., Adams,M.M., Baker,P.W. and Cripps,R.M. (2009) A molecular mechanism of temperature sensitivity for mutations affecting the Drosophila muscle regulator Myocyte enhancer factor-2. *Genetics*, **183**, 107–117.
33. Youn,H.D., Grozinger,C.M. and Liu,J.O. (2000) Calcium regulates transcriptional repression of myocyte enhancer factor 2 by histone deacetylase 4. *J. Biol. Chem.*, **275**, 22563–22567.
34. Mao,Z., Bonni,A., Xia,F., Nadal-Vicens,M. and Greenberg,M.E. (1999) Neuronal activity-dependent cell survival mediated by transcription factor MEF2. *Science*, **286**, 785–790.
35. Wu,H., Naya,F.J., McKinsey,T.A., Mercer,B., Shelton,J.M., Chin,E.R., Simard,A.R., Michel,R.N., Bassel-Duby,R., Olson,E.N. *et al*. (2000) MEF2 responds to multiple calcium-regulated signals in the control of skeletal muscle fiber type. *EMBO J.*, **19**, 1963–1973.
36. Kim,Y., Phan,D., van Rooij,E., Wang,D.Z., McAnally,J., Qi,X., Richardson,J.A., Hill,J.A., Bassel-Duby,R. and Olson,E.N. (2008) The MEF2D transcription factor mediates stress-dependent cardiac remodeling in mice. *J. Clin. Invest.*, **118**, 124–132.
37. Flavell,S.W., Cowan,C.W., Kim,T.K., Greer,P.L., Lin,Y., Paradis,S., Griffith,E.C., Hu,L.S., Chen,C. and Greenberg,M.E. (2006) Activity-dependent regulation of MEF2 transcription factors suppresses excitatory synapse number. *Science*, **311**, 1008–1012.

38. Shalizi,A., Gaudilliere,B., Yuan,Z., Stegmuller,J., Shirogane,T., Ge,Q., Tan,Y., Schulman,B., Harper,J.W. and Bonni,A. (2006) A calcium-regulated MEF2 sumoylation switch controls postsynaptic differentiation. *Science*, **311**, 1012–1017.
39. Yang,Q., She,H., Gearing,M., Colla,E., Lee,M., Shacka,J.J. and Mao,Z. (2009) Regulation of neuronal survival factor MEF2D by chaperone-mediated autophagy. *Science*, **323**, 124–127.
40. McKinsey,T.A., Zhang,C.L. and Olson,E.N. (2002) MEF2: a calcium-dependent regulator of cell division, differentiation and death. *Trends Biochem. Sci.*, **27**, 40–47.
41. Lu,J., McKinsey,T.A., Zhang,C.L. and Olson,E.N. (2000) Regulation of skeletal myogenesis by association of the MEF2 transcription factor with class II histone deacetylases. *Mol. Cell.*, **6**, 233–244.
42. Youn,H.D. and Liu,J.O. (2000) Cabin1 represses MEF2-dependent Nur77 expression and T cell apoptosis by controlling association of histone deacetylases and acetylases with MEF2. *Immunity*, **13**, 85–94.
43. Sparrow,D.B., Miska,E.A., Langley,E., Reynaud-Deonauth,S., Kotecha,S., Towers,N., Spohr,G., Kouzarides,T. and Mohun,T.J. (1999) MEF-2 function is modified by a novel co-repressor, MITR. *EMBO J.*, **18**, 5085–5098.
44. Miska,E.A., Karlsson,C., Langley,E., Nielsen,S.J., Pines,J. and Kouzarides,T. (1999) HDAC4 deacetylase associates with and represses the MEF2 transcription factor. *EMBO J.*, **18**, 5099–5107.
45. Wang,A.H., Bertos,N.R., Vezmar,M., Pelletier,N., Crosato,M., Heng,H.H., Th'ng,J., Han,J. and Yang,X.J. (1999) HDAC4, a human histone deacetylase related to yeast HDA1, is a transcriptional corepressor. *Mol. Cell. Biol.*, **19**, 7816–7827.
46. Lemercier,C., Verdel,A., Galloo,B., Curtet,S., Brocard,M.P. and Khochbin,S. (2000) mHDA1/HDAC5 histone deacetylase interacts with and represses MEF2A transcriptional activity. *J. Biol. Chem.*, **275**, 15594–15599.
47. Lai,M.M., Burnett,P.E., Wolosker,H., Blackshaw,S. and Snyder,S.H. (1998) Cain, a novel physiologic protein inhibitor of calcineurin. *J. Biol. Chem.*, **273**, 18325–18331.
48. Dequiedt,F., Kasler,H., Fischle,W., Kiermer,V., Weinstein,M., Herndier,B.G. and Verdin,E. (2003) HDAC7, a thymus-specific class II histone deacetylase, regulates Nur77 transcription and TCR-mediated apoptosis. *Immunity*, **18**, 687–698.
49. Lu,J., McKinsey,T.A., Nicol,R.L. and Olson,E.N. (2000) Signal-dependent activation of the MEF2 transcription factor by dissociation from histone deacetylases. *Proc. Natl Acad. Sci. USA*, **97**, 4070–4075.
50. Passier,R., Zeng,H., Frey,N., Naya,F.J., Nicol,R.L., McKinsey,T.A., Overbeek,P., Richardson,J.A., Grant,S.R. and Olson,E.N. (2000) CaM kinase signaling induces cardiac hypertrophy and activates the MEF2 transcription factor in vivo. *J. Clin. Invest.*, **105**, 1395–1406.
51. McKinsey,T.A., Zhang,C.L. and Olson,E.N. (2000) Activation of the myocyte enhancer factor-2 transcription factor by calcium/calmodulin-dependent protein kinase-stimulated binding of 14-3-3 to histone deacetylase 5. *Proc. Natl Acad. Sci. USA*, **97**, 14400–14405.
52. Berger,I., Bieniossek,C., Schaffitzel,C., Hassler,M., Santelli,E. and Richmond,T.J. (2003) Direct interaction of ca2+/calmodulin inhibits histone deacetylase 5 repressor core binding to myocyte enhancer factor 2. *J. Biol. Chem.*, **278**, 17625–17635.
53. Wu,Y., Dey,R., Han,A., Jayathilaka,N., Philips,M., Ye,J. and Chen,L. (2010) Structure of the MADS-box/MEF2 domain of MEF2A bound to DNA and its implication for myocardin recruitment. *J. Mol. Biol.*, **397**, 520–533.
54. Creemers,E.E., Sutherland,L.B., Oh,J., Barbosa,A.C. and Olson,E.N. (2006) Coactivation of MEF2 by the SAP domain proteins myocardin and MASTR. *Mol. Cell.*, **23**, 83–96.
55. Gregoire,S., Tremblay,A.M., Xiao,L., Yang,Q., Ma,K., Nie,J., Mao,Z., Wu,Z., Giguere,V. and Yang,X.J. (2006) Control of MEF2 transcriptional activity by coordinated phosphorylation and sumoylation. *J. Biol. Chem.*, **281**, 4423–4433.
56. Ma,K., Chan,J.K., Zhu,G. and Wu,Z. (2005) Myocyte enhancer factor 2 acetylation by p300 enhances its DNA binding activity, transcriptional activity, and myogenic differentiation. *Mol. Cell. Biol.*, **25**, 3575–3582.
57. Han,A., He,J., Wu,Y., Liu,J.O. and Chen,L. (2005) Mechanism of recruitment of class II histone deacetylases by myocyte enhancer factor-2. *J. Mol. Biol.*, **345**, 91–102.
58. Han,A., Pan,F., Stroud,J.C., Youn,H.D., Liu,J.O. and Chen,L. (2003) Sequence-specific recruitment of transcriptional co-repressor Cabin1 by myocyte enhancer factor-2. *Nature*, **422**, 730–734.
59. De Guzman,R.N., Liu,H.Y., Martinez-Yamout,M., Dyson,H.J. and Wright,P.E. (2000) Solution structure of the TAZ2 (CH3) domain of the transcriptional adaptor protein CBP. *J. Mol. Biol.*, **303**, 243–253.
60. Otwinowski,Z. and Minor,W. (1997) Processing of X-ray diffraction data collected in oscillation mode. *Methods Enzymol.*, **276**, 307–326.
61. Santelli,E. and Richmond,T.J. (2000) Crystal structure of MEF2A core bound to DNA at 1.5 A resolution. *J. Mol. Biol.*, **297**, 437–449.
62. McCoy,A.J., Grosse-Kunstleve,R.W., Adams,P.D., Winn,M.D., Storoni,L.C. and Read,R.J. (2007) Phaser crystallographic software. *J. Appl. Cryst.*, **40**, 658–674.
63. Jones,T.A., Zou,J.Y., Cowan,S.W. and Kjeldgaard,M. (1991) Improved methods for building protein models in electron density maps and the location of errors in these models. *Acta Crystallogr. A*, **47(Pt 2)**, 110–119.
64. Emsley,P. and Cowtan,K. (2004) Coot: model-building tools for molecular graphics. *Acta Crystallogr. D Biol. Crystallogr.*, **60**, 2126–2132.
65. Brunger,A.T., Adams,P.D., Clore,G.M., DeLano,W.L., Gros,P., Grosse-Kunstleve,R.W., Jiang,J.S., Kuszewski,J., Nilges,M., Pannu,N.S. *et al.* (1998) Crystallography & NMR system: a new software suite for macromolecular structure determination. *Acta Crystallogr. D Biol. Crystallogr.*, **54**, 905–921.
66. Adams,P.D., Grosse-Kunstleve,R.W., Hung,L.W., Ioerger,T.R., McCoy,A.J., Moriarty,N.W., Read,R.J., Sacchettini,J.C., Sauter,N.K. and Terwilliger,T.C. (2002) PHENIX: building new software for automated crystallographic structure determination. *Acta Crystallogr. D Biol. Crystallogr.*, **58**, 1948–1954.
67. CCP4. (1994) The CCP4 suite: programs for protein crystallography. *Acta Crystallogr. D*, **50**, 760–776.
68. Gregoire,S. and Yang,X.J. (2005) Association with class IIa histone deacetylases upregulates the sumoylation of MEF2 transcription factors. *Mol. Cell. Biol.*, **25**, 2273–2287.
69. De Luca,A., Severino,A., De Paolis,P., Cottone,G., De Luca,L., De Falco,M., Porcellini,A., Volpe,M. and Condorelli,G. (2003) p300/cAMP-response-element-binding-protein ('CREB')-binding protein (CBP) modulates co-operation between myocyte enhancer factor 2A (MEF2A) and thyroid hormone receptor-retinoid X receptor. *Biochem. J.*, **369**, 477–484.
70. Miller,M., Dauter,Z., Cherry,S., Tropea,J.E. and Wlodawer,A. (2009) Structure of the Taz2 domain of p300: insights into ligand binding. *Acta Crystallogr. D Biol. Crystallogr.*, **65**, 1301–1308.
71. Angelelli,C., Magli,A., Ferrari,D., Ganassi,M., Matafora,V., Parise,F., Razzini,G., Bachi,A., Ferrari,S. and Molinari,S. (2008) Differentiation-dependent lysine 4 acetylation enhances MEF2C binding to DNA in skeletal muscle cells. *Nucleic Acids Res.*, **36**, 915–928.